

*Physics**Physics Research Publications*

---

*Purdue University**Year 2003*

---

Measurement of leading Lambda's and  
Delta(++)'s in p+Pb collisions at 19  
GeV/c

K. N. Barish, S. Batsouli, S. J. Bennett, M. Bertaina, A. Chikanian, T. M. Cormier, P. Fachini, B. Fadem, S. Q. Feng, L. E. Finch, N. K. George, S. V. Greene, P. Haridas, J. C. Hill, A. S. Hirsch, R. Hoversten, H. Z. Huang, H. Jaradat, T. Lainis, J. G. Lajoie, Q. Li, L. S. Liu, H. Long, C. Maguire, R. D. Majka, T. E. Miller, M. G. Munhoz, J. L. Nagle, A. Petridis, I. A. Pless, N. T. Porile, C. A. Pruneau, M. S. Z. Rabin, J. D. Reid, A. Rose, J. Sandweiss, R. P. Scharenberg, A. J. Slaughter, A. Tai, G. Van Buren, F. K. Wohn, Z. Xu, and E. Yamamoto

This paper is posted at Purdue e-Pubs.

[http://docs.lib.purdue.edu/physics\\_articles/495](http://docs.lib.purdue.edu/physics_articles/495)

**Measurement of leading  $\Lambda$ 's and  $\Delta^{++}$ 's in  $p$ +Pb Collisions at 19 GeV/c**

K. N. Barish,<sup>2</sup> S. Batsouli,<sup>11</sup> S. J. Bennett,<sup>10</sup> M. Bertaina,<sup>6,\*</sup> A. Chikanian,<sup>11</sup> T. M. Cormier,<sup>10</sup> P. Fachini,<sup>10,†</sup> B. Fadem,<sup>4</sup> S. Q. Feng,<sup>1</sup> L. E. Finch,<sup>11</sup> N. K. George,<sup>11</sup> S. V. Greene,<sup>9</sup> P. Haridas,<sup>6</sup> J. C. Hill,<sup>4</sup> A. S. Hirsch,<sup>7</sup> R. Hoversten,<sup>4</sup> H. Z. Huang,<sup>1</sup> H. Jaradat,<sup>10</sup> T. Lainis,<sup>8</sup> J. G. Lajoie,<sup>4</sup> Q. Li,<sup>10</sup> L. S. Liu,<sup>1</sup> H. Long,<sup>1</sup> C. Maguire,<sup>9</sup> R. D. Majka,<sup>11</sup> T. E. Miller,<sup>9</sup> M. G. Munhoz,<sup>10</sup> J. L. Nagle,<sup>3</sup> A. Petridis,<sup>4</sup> I. A. Pless,<sup>6</sup> N. T. Porile,<sup>7</sup> C. A. Pruneau,<sup>10</sup> M. S. Z. Rabin,<sup>5</sup> J. D. Reid,<sup>9</sup> A. Rose,<sup>9</sup> J. Sandweiss,<sup>11</sup> R. P. Scharenberg,<sup>7</sup> A. J. Slaughter,<sup>11</sup> A. Tai,<sup>1</sup> G. Van Buren,<sup>1,†</sup> F. K. Wohn,<sup>4</sup> Z. Xu,<sup>11,†</sup> and E. Yamamoto<sup>1</sup>

(E941 Collaboration)

<sup>1</sup>University of California at Los Angeles, Los Angeles, California 90095<sup>2</sup>University of California at Riverside, Riverside, California 92521<sup>3</sup>Columbia University, Nevis Laboratory, Irvington, New York 10533<sup>4</sup>Iowa State University, Ames, Iowa 50011<sup>5</sup>University of Massachusetts, Amherst, Massachusetts 01003<sup>6</sup>Massachusetts Institute of Technology, Cambridge, Massachusetts 02139<sup>7</sup>Purdue University, West Lafayette, Indiana 47907<sup>8</sup>United States Military Academy, West Point, New York 10996<sup>9</sup>Vanderbilt University, Nashville, Tennessee 37235<sup>10</sup>Wayne State University, Detroit, Michigan 48201<sup>11</sup>Yale University, New Haven, Connecticut 06520

(Received 11 March 2002; published 15 January 2003)

We present the first comprehensive measurement of leading  $\Lambda$ 's and  $\Delta^{++}$ 's in  $p$ +Pb collisions at 19 GeV/c using the E941/E864 spectrometer at the AGS. In comparison with the measurement of leading protons and neutrons using the same spectrometer, it is found that the cross section for baryon flavor change is large and strongly depends on rapidity, which is very different from the expectation of simple diquark-quark fragmentation of the incident proton. A suppression of leading  $\Lambda$  production in the forward rapidity region compared with nonstrange leading baryons is also observed. The relative probability of the projectile proton fragmentation into a  $\Delta^{++}$  versus into a neutron is found to be about 35% in the region of  $2.7 \leq y \leq 3.1$ . We will discuss the impact of these results on the dynamics of baryon fragmentation and baryon number transport in nuclear collisions.

DOI: 10.1103/PhysRevC.67.014902

PACS number(s): 25.40.-h, 13.85.Ni, 25.40.Kv, 25.75.-q

**I. INTRODUCTION**

Leading baryons in  $p$ + $A$  collisions, which carry the baryon quantum numbers of the incident protons, reflect both the dynamics for the baryon number transport mechanism and indirectly the energy partition between leading particles and produced particles. At Alternating Gradient Synchrotron (AGS) energies, the baryon pair production cross section is small, and baryons in the forward proton hemisphere in the center-of-mass system should, to a very good approximation, carry the incident baryon number and are regarded as leading baryons. In the phenomenological models this was described as incident proton fragmentation into pieces, one of which emerges as a leading baryon because of baryon number conservation. Schematically we will describe the baryon fragmentation processes based on the gluon junction configuration of the baryon wave function. The gluon junction configuration, arising from gauge invariance [1,2], consists

of three gluon strings from one junction where the other ends of the strings are connected to valence quarks. Thus depending on the number of broken gluon strings the fragmentation processes are divided into the following: one gluon string is broken where the emerging baryon contains a diquark of the incident proton (diquark-quark fragmentation), two gluon strings are simultaneously broken where the emerging baryon contains one valence quark (three-quark fragmentation), and all three gluon strings are broken where the emerging baryon is formed from the gluon junction (gluon junction fragmentation) and contains no valence quark. In these fragmentation schemes, the leading particle spectra may be related to the structure of valence quarks in the incident proton and the average momentum of the leading baryon decreases as the number of projectile valence quarks in the emerging baryon decreases.  $p$ + $A$  collisions provide a unique means to study the dynamics for baryon number transport and baryon energy loss in nuclear collisions.

Previous theoretical works were mostly based on very limited knowledge of proton fragmentation [3]. Early models of relativistic heavy ion collisions, e.g. FRITIOF [4], VENUS [5], and HIJING [6], were constrained with the diquark-quark fragmentation scheme only, which could not produce the baryon stopping seen in experimental data in relativistic  $p$

\*Present address: Dipartimento di Fisica Generale, Universita' di Torino, Italy.

†Present address: Brookhaven National Laboratory, Upton, New York 11973.

+A and A+A collisions. More recent theoretical works [7,8] have tried to implement three-quark and/or gluon junction fragmentation schemes in order to produce stronger baryon stopping. It was also found that the three-quark and gluon junction fragmentation enhances the yield of strange particles. No theoretical framework has been established so far to systematically address all these fragmentation schemes. In fact, previous experimental measurements were not sufficient to constrain all the fragmentation functions and there is no conclusive experimental evidence for baryon production through gluon junction fragmentation. The lack of a comprehensive experimental study of the fragmentation functions also introduces large uncertainties in the model calculations of the atmospheric neutrino flux [9], which is an important quantity for exploring neutrino oscillations. Recent  $p+A$  experiments were intended to better constrain theoretical models [10,11].

The flavor of leading baryons in  $p+A$  collisions is sensitive to proton fragmentation schemes. A comprehensive study of all leading baryons will help us disentangle different fragmentation processes. In a simple diquark fragmentation scheme, the emerging leading baryon may contain either a  $uu$  or a  $ud$  diquark from the incident proton. The  $ud$  diquark may be shared by either a leading proton or a leading neutron while the  $uu$  diquark can only appear in a leading proton (resonance production is not considered here, which will be discussed below). The diquark fragmentation scheme would thus predict a proton-to-neutron ratio of 2 for leading baryon production. On the other hand, the gluon junction scheme will yield an equal number of leading protons and neutrons in the final state in  $p+A$  collisions. In addition, since a  $\Lambda$  and a neutron have a  $ud$  quark pair in common the yield difference would reflect the relative probability between baryons with an  $s$  or a  $d$  quark in the wave function. Therefore, the ratio of  $\Lambda$ 's to neutrons measures the strangeness suppression factor in fragmentation.

The leading baryons may be produced directly or through resonance decays. We note that resonance production may play an important role in isospin exchange reactions at AGS energies. However, based on a FRITIOF calculation, the  $\Delta(1232)$  excitation seems to yield a proton-to-neutron ratio similar to that from diquark fragmentation. Because of the strong interaction between the proton and pion,  $\Delta$  resonances can also be formed in the final state, instead of from direct fragmentation processes. However, there are few experimental measurements to quantify the  $\Delta$  contribution in  $p+A$  collisions.

## II. EXPERIMENTAL DESCRIPTION

In this paper, we report our comprehensive measurement of leading  $\Lambda$ 's and  $\Delta^{++}$ 's from  $p+Pb$  collisions at 19 GeV/c using the E941 spectrometer. The E941 experiment used the E864 spectrometer with modifications for study of  $p+A$  collisions. Prominent features of this spectrometer include open geometry optimized for high rapidity particle acceptance in the forward direction, a hadronic calorimeter for the neutral particle measurement, and a high data collection rate. Those features make E941 a unique experi-

ment to study leading baryon production in  $p+A$  collisions at AGS energies. The experimental setup of E941 was introduced in Ref. [10]. The tracking detectors are located behind two dipole magnets and consist of three segmented scintillating hodoscope arrays and two straw tube chambers. The track rigidities were obtained from the curvature of the track as it traversed the dipole magnetic field, and the typical tracking momentum resolution is about 6%. The hadronic calorimeter is situated at the end of the spectrometer, approximately 27 m from the target. The tracking system worked as a charged track veto for the measurement of neutral particles. The interaction trigger (level 0) was provided by a multiplicity counter, and a spectrometer trigger (level 1) required that a minimum of 0.3 GeV energy be deposited in any of the calorimeter towers.

The E941 experiment was run at two magnetic field settings +0.2 T and -0.2 T, which optimized the acceptance for positive and negative particles, respectively. About  $40 \times 10^6$  events taken with the spectrometer trigger were used in this analysis, about half from the -0.2 T field run and the rest from the +0.2 T field run. The spectrometer trigger enhanced the number of particles in our data sample by approximately a factor of 10. Our interaction trigger recorded about 97% of the total inelastic interactions [10] for the Pb target at 19 GeV/c. Taking into account interactions triggered by  $\delta$  ray electrons from the target and from nontarget sources, approximately  $197 \times 10^6$   $p+Pb$  interactions are sampled.

The analyses for leading protons and neutrons have been described in [10]. For the  $\Lambda$  and  $\Delta^{++}$  analyses the event mixing method was used for subtraction of the combinatorial background. This method has been successfully used in the E864 experiment to extract yields of unstable resonance nuclei and  $\Lambda$ 's in nucleus-nucleus collisions [12]. The events with at least one positive track and one negative track in the spectrometer are used for  $\Lambda$  reconstruction (sample I) and the events with at least two positive tracks are used for  $\Delta^{++}$  reconstruction (sample II). The event mixing is done sepa-

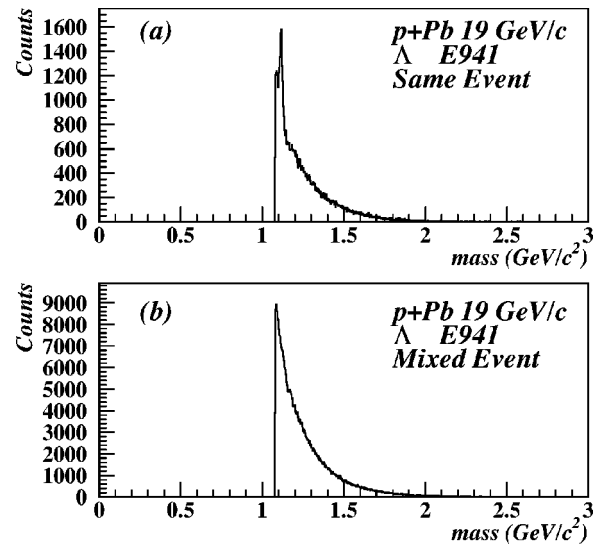


FIG. 1. The mass spectra of unlike sign pairs from the same events (a) and the mixed events (b) at -0.2 T for the  $\Lambda$  analysis.

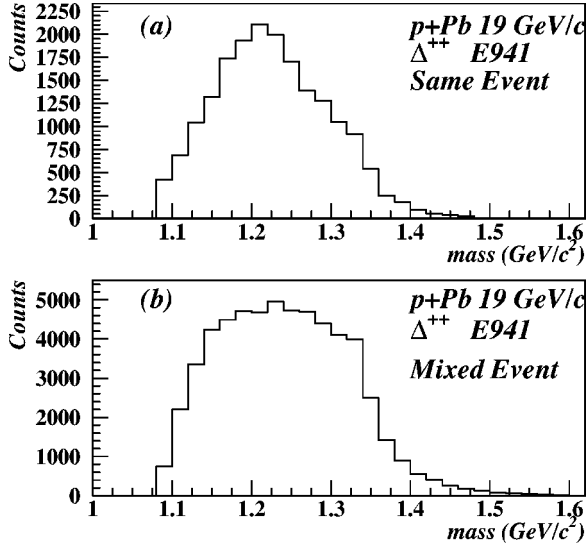


FIG. 2. The mass spectra of positive sign pairs from the same events (a) and the mixed events (b) at  $-0.2$  T for the  $\Delta^{++}$  analysis.

rately in sample I for  $\Lambda$  background and in sample II for  $\Delta^{++}$  background. It was also required that the hit positions of two tracks on any hodoscope plane should be separated by at least two hodoscope slats. In addition, for the  $\Delta^{++}$  background, two positive tracks of two different events are not paired if each of them has a momentum larger than 10 GeV/c, since this would violate energy-momentum conservation. In this case, the two positive tracks are mostly protons. The above procedure assures that the pairs from the mixed events reproduce energy and momentum distributions similar to those of the same event pairs.

We assumed the proton mass for the positive track with the largest momentum in an event and the  $\pi$  mass for all other tracks. Then, the invariant mass spectra of the unlike sign pairs and positive sign pairs were calculated from the same events and mixed events for the  $\Lambda$  and  $\Delta^{++}$  analyses, respectively, as shown in Figs. 1 and 2. The  $(p, \pi)$  invariant mass distribution for signal  $D(M)_{signal}$  can be extracted from the invariant mass distributions of the same event pairs [ $D(M)_{same}$ ] and the mixed event pairs [ $D(M)_{mix}$ ] by

$$D(M)_{signal} = D(M)_{same} - \frac{N_{same} - N_{signal}}{N_{mix}} D(M)_{mix}, \quad (1)$$

where  $N_{signal}$ ,  $N_{same}$ , and  $N_{mix}$  are the number of signal, the same event pairs, and the mixed event pairs, respectively. As a result of the long tail of the  $\Delta$  resonance, it is not always possible to normalize  $D(M)_{mix}$  to  $D(M)_{same}$  at large values of  $M$ , where the correlated pair vanishes. We then try to solve Eq. (1) through an iterative algorithm. We subtract the invariant mass histogram of the mixed event pairs scaled by  $N_{same}/N_{mix}$  from the invariant mass histogram of the same event pairs. The resulting invariant mass histogram has zero net entries, and the sum of its positive contents in the region of the ( $\Delta$ ) mass is called  $N_R$ . We repeat the above calculation with a new scale factor  $(N_{same} - N_R)/N_{mix}$  for the normalization of the mixed event histogram. A new  $N_R$  is then obtained and the iteration continues until the change of  $N_R$  of two adjacent steps becomes smaller than a given cut. This procedure is applicable for particles whose properties and detector responses are understood from simulations.

The invariant mass spectra after the subtraction of the combinatorial background are shown in Fig. 3(a) for  $\Lambda$  and in Fig. 3(b) for  $\Delta^{++}$  from the  $-0.2$  T field run. The subtracted invariant mass spectra still have some residual background due to correlated pairs in the same event sample. The statistical errors in Figs. 3(a) and 3(b) are calculated from Eq. (1). We extracted the raw yield by fitting the residual background with an exponential function and the signal with a Gaussian function, as seen in Fig. 3. In case of the  $\Lambda$  analysis, another Gaussian function (with its mean and width fixed to those of  $\Delta^{++}$ ) was also used to fit  $\Delta^0$ . One could see that as a result of the narrow width of  $\Lambda$ ,  $\Delta^0$  contamination to the  $\Lambda$  signal is small ( $\sim 3\%$ ) and can be easily subtracted as part of the residual background. We do not study  $\Delta^0$  in this article partly because  $\Delta^0$  decays into a  $(p, \pi^-)$  pair only 33% of the time and partly because the higher mass resonance  $N^*(1440)$  can also decay into a  $(p, \pi^-)$  pair and complicates the  $\Delta^0$  analysis while  $\Delta^{++}$  decays into a  $(p, \pi^+)$  pair 100% of the time. The exponential function was chosen because the extracted signals matched well with those from Monte Carlo simulations with detector resolutions. The simulations also showed that the Gaussian function fits the reconstructed  $\Delta^{++}$  mass spectra better than the Breit-Wigner function, presumably due to our limited  $\Delta^{++}$  acceptance which varies with mass. No significant mass shift of  $\Delta^{++}$  was seen in our data unlike that reported in A+A collisions at lower energy [13]. However, the E941 accep-

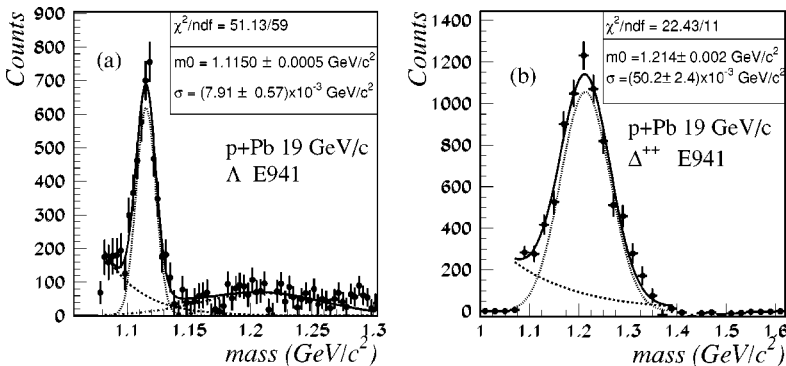


FIG. 3. The mass spectrum of  $\Lambda$  (a) and  $\Delta^{++}$  (b) from  $-0.2$  T data. The background is fit with an exponential function and the signal with a Gaussian function. In (a), another Gaussian function was also used to fit  $\Delta^0$ . The  $\chi^2$  per degree of freedom and fitted parameters for the signal are given in the figure.

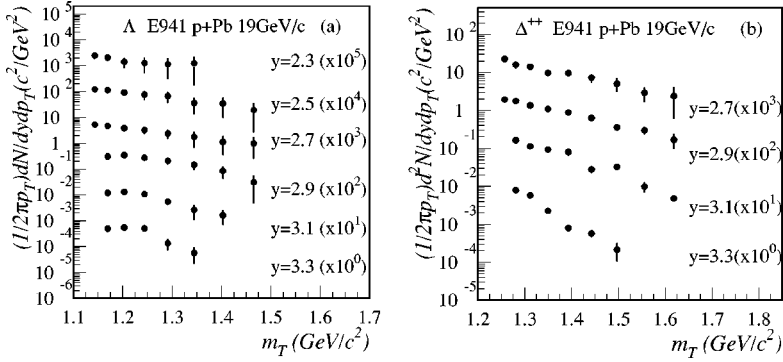


FIG. 4. Leading  $\Lambda$  and leading  $\Delta^{++}$  invariant multiplicities in  $p + \text{Pb}$  collisions at 19 GeV/c as a function of transverse mass for different rapidity bins. The multiplicity of each rapidity bin is multiplied by a successive factor of 10.

tance for the  $\Delta^{++}$  is changed dramatically over the  $\Delta^{++}$  mass range, which makes E941 relatively insensitive to a small mass shift.

From all the data, 4059  $\Lambda$ 's in the region of  $1.10 \text{ GeV}/c^2 < \text{mass} < 1.13 \text{ GeV}/c^2$  and 17058  $\Delta^{++}$ 's in the region of  $1.10 \text{ GeV}/c^2 < \text{mass} < 1.40 \text{ GeV}/c^2$  were counted. We then divided the  $p_T$ - $y$  phase space of  $\Lambda$  ( $\Delta^{++}$ ) into bins of 100 MeV/c in  $p_T$  and 0.2 in rapidity, separately for the +0.2 T and -0.2 T runs. The background subtraction was done bin by bin to extract the signal in each bin.

By embedding Monte Carlo simulated decays in real data events, we calculated the geometry acceptances and reconstruction efficiencies for measurements of  $\Lambda$  and  $\Delta^{++}$  using the E864/E941 spectrometer. For the -0.2 T field setting, typical geometry acceptances for  $\Lambda$  are 0.10% at  $y = 2.3$ ,  $p_T = 0.4 \text{ GeV}/c$  and increase to 2.80% at  $y = 3.3$ ,  $p_T = 0.4 \text{ GeV}/c$ , and for  $\Delta^{++}$  are 0.40% at  $y = 2.7$ ,  $p_T = 0.5 \text{ GeV}/c$  and increase to 1.80% at  $y = 3.3$ ,  $p_T = 0.5 \text{ GeV}/c$ . For the +0.2 T field setting, the numbers are 0.04% at  $y = 2.3$ ,  $p_T = 0.4 \text{ GeV}/c$  and 1.10% at  $y = 3.1$ ,  $p_T = 0.4 \text{ GeV}/c$  for  $\Lambda$  and are 0.61% at  $y = 2.7$ ,  $p_T = 0.5 \text{ GeV}/c$  and 3.40% at  $y = 3.3$ ,  $p_T = 0.5 \text{ GeV}/c$  for  $\Delta^{++}$ . The reconstruction efficiencies are about 60% for both  $\Lambda$  and  $\Delta^{++}$  at both field settings. In addition, the hardware inefficiency of the tracking system, which was not included in the calculation of the reconstruction efficiencies, was found to be 90% using real data. The invariant multiplicities from the two fields were found to be in good agreement with each other and the differences were included in the estimate for systematic errors. In addition, a 5% error in the overall normalization of the invariant multiplicities due to the calculation of the  $\delta$ -ray interaction rate was also included in the systematic errors.

### III. RESULTS AND DISCUSSION

The measured leading  $\Lambda$  and leading  $\Delta^{++}$  invariant multiplicities in  $p + \text{Pb}$  collisions at 19 GeV/c are shown in Fig.

TABLE I. Inverse slope parameters of  $\Lambda$  and  $\Delta^{++}$  in MeV in  $p + \text{Pb}$  at 19 GeV/c.

Rapidity	2.3	2.5	2.7	2.9	3.1	3.3
$\Lambda$	$159 \pm 58$	$159 \pm 31$	$157 \pm 32$	$146 \pm 25$	$110 \pm 17$	$82 \pm 5$
$\Delta^{++}$			$137 \pm 24$	$136 \pm 32$	$88 \pm 6$	$56 \pm 3$

4. We fit the spectra with a Boltzmann distribution in transverse mass,  $Am_T \exp(-m_T/T)$ , for obtaining  $dN/dy$ . The inverse slope parameters  $T$  for  $\Lambda$  and  $\Delta^{++}$ , obtained from the fitting, are listed in Table I. One could see that the slope parameters of  $\Lambda$  and  $\Delta^{++}$  are comparable in a given rapidity bin, but they may be systematically higher than those for protons and neutrons [10], which is consistent with the measurements in  $p + \bar{p}$  collisions where the mean transverse momenta of produced particles were found to increase with mass [14]. However, the current experimental uncertainties do not allow us to make a definite statement on this matter.

$dN/dy$  for protons, neutrons,  $\Lambda$ 's, and  $\Delta^{++}$ 's are shown in Fig. 5. It was found that the E941  $\Lambda$  result, when plotted as a function of light cone variable  $x_+ \equiv (E + p_z)/(E + p_z)_{\text{beam}}$ , is in good agreement with the E910 measurement in  $p + \text{Au}$  collisions at 17.5 GeV/c [15], but extends to the higher  $x_+$  region. The  $\Lambda$  and  $\Delta^{++}$  results are also compared with the RQMD predictions [7] in Fig. 5. Note that  $dN/dy$  for protons and neutrons has been corrected for  $\Lambda$  feeddown. The measured leading baryon yields decrease with increasing rapidity, but the  $\Lambda$  yield decreases much faster than that for nonstrange leading baryons. RQMD reproduces the measured  $\Lambda$  yield at  $y = 2.3$  while it overestimates the E941 data, especially the  $\Lambda$  yield, in the forward rapidity region. The decreased yields of leading baryons with rapidity may be considered as due to a kinematic constraint from four-momentum conservation. For example, due to the associated production of strange particles, it needs about 700 MeV threshold energy to produce a  $\Lambda$  through a reaction  $NN$

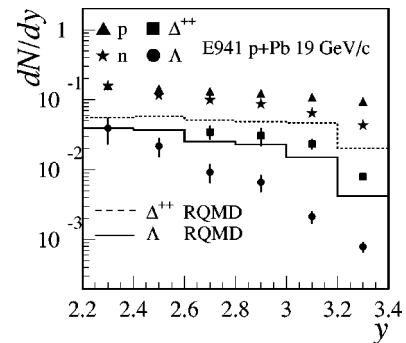


FIG. 5.  $dN/dy$  for protons, neutrons,  $\Lambda$ 's, and  $\Delta^{++}$ 's in  $p + \text{Pb}$  collisions at 19 GeV/c and the  $\Lambda$  and  $\Delta^{++}$  results are compared with RQMD predictions. Note that the beam rapidity is 3.7 at 19 GeV/c.



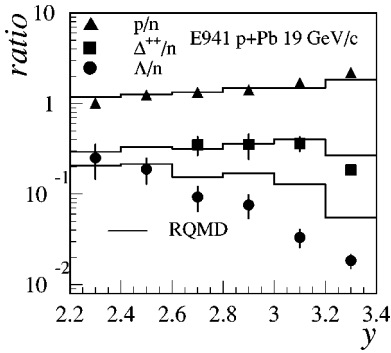


FIG. 6. Relative yields of protons,  $\Delta^{++}$ 's, and  $\Lambda$ 's with respect to neutrons as a function of rapidity in  $p$ +Pb collisions at 19 GeV/ $c$  compared with RQMD predictions.

$\rightarrow \Lambda KN$ , thereby making it hard to produce a  $\Lambda$  in the large rapidity region. However, the phase space effects alone obviously cannot explain all the discrepancy between our data and the RQMD predictions since the four-momentum conservation has already been properly implemented into RQMD. The dynamics of proton fragmentation and strange quark hadronization for  $\Lambda$  formation should play a role. To further quantify the effect from the kinematic constraint would require a full acceptance detector to measure exclusive channels. Note that the amount of  $\Lambda$  production in the very forward rapidity region is only a small fraction of the total. This difference will not lead to a large difference in total  $\Lambda$  multiplicity between RQMD and the experimental data. In fact, RQMD is shown to reproduce measured  $\Lambda$  yields at midrapidity in Au+Au collisions reasonably well [16]. However, the E941 results point to a deficiency in the RQMD fragmentation scheme for baryon production in the beam fragmentation region. This is consistent with the previous observation that RQMD overpredicts the baryon yields in the very forward rapidity region in  $p+A$  and  $A+A$  collisions at the AGS [10,17].

In Fig. 6, we plot the ratios of  $\Lambda$  and  $\Delta^{++}$  yields to the neutron yield. The proton-to-neutron ratio and RQMD predictions are also shown for comparison. Figure 6 shows that the  $p/n$  ratio increases from 1 at  $y=2.3$  to above 2 at  $y=3.3$ ,  $\Lambda/n$  decreases rapidly from  $0.26 \pm 0.13$  at  $y=2.3$ , and  $\Delta^{++}/n$  stays almost flat (about 35%) in the region of  $2.7 \leq y \leq 3.1$ . Although the RQMD model overpredicts yields of the leading baryons in the forward rapidity region, the calculated  $p/n$  and  $\Delta^{++}/n$  ratios seem to agree with the E941 data. However, the  $\Lambda/n$  ratio from RQMD shows a rapidity dependence inconsistent with the data, which may again indicate that the new fragmentation schemes are needed in order to understand the current measurements.

The E941  $p/n$  ratio indicates that the simple diquark-quark fragmentation scheme, which predicts a proton-to-neutron ratio of 2, is unlikely to be the only relevant process in  $p+A$  collisions for leading baryons in our rapidity acceptance. In order to explain a  $p/n$  ratio of unity we have to include other fragmentation schemes, perhaps even dominat-

ing over the diquark-quark fragmentation in the relevant kinematic region, such as three-quark fragmentation and/or gluon junction fragmentation. Our measurement is a unique constraint to these additional fragmentation functions. The significant presence of three-quark and gluon junction fragmentation processes would indicate that the incident proton is very brittle in nuclear collisions and is likely to fragment into pieces.

The ratio of  $\Lambda/n$  is a sensitive measure of strangeness suppression in proton fragmentation. In Fig. 6, the  $\Lambda$  production in the very forward rapidity region shows a stronger suppression compared with nonstrange leading baryons. The strong rapidity dependence of the strangeness suppression may indicate that such suppression is sensitive to the fragmentation schemes. For example, the diquark fragmentation, which dominates the leading baryon production in the large rapidity region, may have greater strangeness suppression than the three-quark and gluon junction fragmentation scheme. The E910  $\Lambda$  data also show that the enhancement of the  $\Lambda$  yield with number of collisions is faster than  $p+p$  extrapolation of the wounded nucleon model, which may imply that the fraction of the three-quark and gluon junction fragmentation increases with the number of collisions.

$p+A$  collisions provide a unique means to study the dynamics of baryon fragmentation, baryon number transport, and hyperon production. We have presented the first comprehensive measurement of leading  $\Lambda$ 's and  $\Delta^{++}$ 's in  $p+Pb$  collisions at 19 GeV/ $c$  with the E846/E941 spectrometer. The comparison of our results with RQMD and with diquark-quark fragmentation demonstrates significant deficiencies in the current understanding of the baryon fragmentation processes. Theoretical understanding of three-quark and gluon junction fragmentation processes needs to be developed. These studies will have an important impact on understanding nucleus-nucleus collisions at the Relativistic Heavy Ion Collider (RHIC). The measurement of baryon and antibaryon production at RHIC has shown that the net baryon density at midrapidity is small, but finite [18]. These net baryons are transported to midrapidity from the beam through a gap of five units of rapidity. In order to understand the dynamics of baryon number transport and, in particular, to possibly study the gluon junction interaction process, we should measure exclusive leading charged and neutral particles in the proton hemisphere in  $p+A$  collisions at RHIC. A gluon junction interaction event is likely to produce a topology with exclusive leading mesons from valence quarks. Comprehensive measurement of all leading particles will provide more constraints on the dynamics of baryon number transport and energy deposition at midrapidity in nuclear collisions.

#### ACKNOWLEDGMENTS

We gratefully acknowledge the excellent support of the AGS staff. This work was supported in part by grants from the U.S. Department of Energy's High Energy and Nuclear Physics Divisions and the U.S. National Science Foundation.

- [1] G. C. Rossi and G. Veneziano, Nucl. Phys. **B123**, 507 (1977).
- [2] D. Kharzeev, Phys. Lett. B **378**, 238 (1996).
- [3] L. Van Hove, Z. Phys. C **9**, 145 (1981); C. Iso and S. Iwai, *ibid.* **11**, 103 (1981); T. K. Choi, M. Maruyama, and F. Takagi, Phys. Rev. C **55**, 848 (1997).
- [4] B. Andersson, G. Gustafson, and B. Nilsson-Almqvist, Nucl. Phys. **B281**, 289 (1987).
- [5] K. Werner, Phys. Rev. D **39**, 780 (1989).
- [6] X. N. Wang and M. Gyulassy, Phys. Rev. D **44**, 3501 (1991).
- [7] H. Sorge, Z. Phys. C **67**, 479 (1995).
- [8] A. Capella and B. Kopeliovich, Phys. Lett. B **381**, 325 (1996); S. E. Vance, M. Gyulassy, and X. N. Wang, *ibid.* **443**, 45 (1998).
- [9] R. Engel, T. K. Gaisser, and T. Stanev, Phys. Lett. B **472**, 113 (2000).
- [10] E941 Collaboration, K. N. Barish *et al.*, Phys. Rev. C **65**, 014904 (2002).
- [11] E910 Collaboration, B. A. Cole, Nucl. Phys. **A661**, 366 (1999).
- [12] E864 Collaboration, T. A. Armstrong *et al.*, Phys. Rev. C **65**, 014906 (2002); S. Batsouli, Ph.D. thesis, Yale University, 2001.
- [13] FOPI Collaboration, M. Eskef *et al.*, Eur. Phys. J. A **3**, 335 (1998).
- [14] UA5 Collaboration, G. J. Alner *et al.*, Phys. Rep. **154**, 247 (1987).
- [15] E910 Collaboration, I. Chemakin *et al.*, Phys. Rev. C **60**, 024902 (1999); Ron Soltz, J. Phys. G **27**, 319 (2001).
- [16] S. Ahmad *et al.*, Phys. Lett. B **382**, 35 (1996).
- [17] E864 Collaboration, T. A. Armstrong *et al.*, Phys. Rev. C **60**, 064903 (1999); E896 Collaboration, S. Albergo *et al.*, Phys. Rev. Lett. **88**, 062301 (2002).
- [18] STAR Collaboration, C. Adler *et al.*, Phys. Rev. Lett. **86**, 4778 (2001).